

Network Pharmacology Study to Reveal Underlying Mechanisms, Targets, and Bioactives of *Aralia Cordata* Against Obesity

Ki Kwang Oh (✉ nivima07@kangwon.ac.kr)
Kangwon National University

Research Article

Keywords: Aralia cordata, obesity, network pharmacology, Insulin resistance, IL6, Andrographolide

Posted Date: March 15th, 2022

DOI: <https://doi.org/10.21203/rs.3.rs-1429030/v1>

License: © ⓘ This work is licensed under a Creative Commons Attribution 4.0 International License. [Read Full License](#)

Abstract

Aralia cordata (AC) has been used as anti-obesity herbal plants by Chinese, Japanese, and Korean, but its active chemical constituents, mechanism(s), and targets have not been documented completely. We aimed to investigate significant phytochemicals, pathways, and targets of AC against obesity via network pharmacology. The phytochemicals from AC were identified by Gas Chromatography Mass Spectrum (GC-MS) and were screened subsequently by Lipinski's rule. The compound-target relationships were retrieved by analyzing SwissTargetPrediction (STP), SEA search server. Then, obesity-related targets were identified by public bioinformatics and final overlapping targets were selected by Ven diagram. Next, we constructed and visualized protein-to-protein interaction (PPI) networks, bubble chart, and pathways-targets-compounds (PTC) networks by RPackage. Furthermore, we utilized the Autodock Tools to perform molecular docking test (MDT) on the bioactives and key targets to validate the network pharmacological results. We confirmed a total of 43 compounds from AC via GC-MS and 40 final targets regarding obesity. The PPI networks analysis revealed IL6 as a key target, and a bubble chart showed that inactivation of Insulin resistance might be the uppermost pathway for anti-obesity. We identified that the AC phytochemicals was contributed to synergistic effects (multi-pathway, multi-target) to alleviate obesity through PTC analysis. We conducted MDT to verify the most significant compound on a key target (IL6), thereby, confirmed Andrographolide as a key compound of AC on obesity. Overall, we elucidated a key pathway, target, and bioactive of AC against obesity, suggesting significant pharmacological basis for further clinical trials.

Introduction

Obesity is a severe medical condition that can cause diverse complications such as hypertension, diabetes, atherosclerosis, heart disease and even cancer [1]. The World Health Organization (WHO) announced that more than 1.9 billion adults in 2016 are subjected to overweight (around 40% of the population) and over 650 million (around one-quarter of the population) were categorized into obesity [2]. Obesity is described by the inappropriate accumulation of fat in the body, causing energy imbalance, change of appetite hormones, and even insulin resistance [3,4]. The clinical standard of obesity is that Body Mass Index (BMI) is equal to 30.0 or greater [5]. Obesity can occur at all ages, especially, can aggravate physical as well as mental condition [6]. The most effective therapeutic strategy against obesity is to directly inhibit absorption of fat in the body, also, to administer appetite suppressants [7]. A study reported the number of five anti-obesity drugs can be used for long term in spite of some adverse effects (oily stools, insomnia, anxiety, depression, vomiting, and dry mouth): (1) Orlistat (the inhibition of lipid absorption), (2) Phentermine/topiramate (suppressor of appetite), (3) Naltrexon/bupropion (suppressor of appetite), (4) Liraglutide (increase in satiety), and (5) Lorcaserin (reduction in food intake) [8].

Obesity is associated with multiple pathways, a single medication might have limited effects and thus a high dose can cause unexpected side effects [8,9]. Therefore, a report suggested that combination drug therapy with complementary mechanism of action might be an optimal therapeutic by controlling actions on distinct pathways on obesity, which could enhance the efficacy of weight management as well as maintaining safety [10]. Particularly, natural herbal plants with diverse bioactive compounds might be good resources to be expected synergistic effect with minimal side effects against obesity [11]

Of these, methanolic extraction of *Aralia cordata* (AC) can be used to alleviate lipid metabolism disorders, which could be beneficial in preventing their even complications [12].

However, there has been no integrative research on the efficacy of AC on obesity. Furthermore, the bioactives, targets, and mechanism of action of AC on obesity have not been established. Thus, we investigated the multiple components (bioactives, targets, and pharmacological mechanism) via network pharmacology.

Network pharmacology is a systemic methodology to uncover multiple elements such as compounds, targets, diseases, and pathways [13]. Network pharmacology can decode the mechanism of compounds action with comprehensive viewpoint, which sheds light on the paradigm shift from "one target, one compound" to "multiple targets, multiple pathways" [14].

Additionally, the rapid development of bioinformatics, system biology, network biology, and integrating network pharmacology is a rising analytical approach toward cost-efficient drug discovery [15]. The network pharmacology concept is an effective application to find potential drugs for the treatment of obesity related to metabolic disorders [16]. From this viewpoint, we aimed to construct a new methodology and notion to uncover anti-obesity efficacy on AC. Firstly, compounds from AC were identified by Gas Chromatography Mass Spectrum (GC-MS) and confirmed by Lipinski's rule. Targets associated with the compounds or obesity related targets were retrieved by public bioinformatics databases, and overlapping final targets were selected by Ven diagram plotter. Secondly, Protein-Protein Interaction (PPI) networks on the final overlapping targets were built by RPackage. We confirmed a key target through topological analysis on degree centrality (DC), and betweenness centrality (BC). Then, a bubble chart represented significant pathways based on the Rich Factor. Thirdly, relationships between pathways, targets, and compounds were constructed by RPackage. Lastly, we performed Molecular Docking Test (MDT) to verify the affinity between targets and ligands related to pathways of AC on obesity. The workflow of this study is represented in Fig. 1.

Results

Profiling of chemical constituents from AC

A total of 43 chemical constituents were identified by GC-MS (Figure 2), which were profiled compound name, PubChem ID, retention time (RT), area, and taxonomic classification (Table 1). The identified all 43 compounds were confirmed by Lipinski's rule (Molecular Weight \leq 500 g/mol; Moriguchi octanol-water partition coefficient \leq 4.15; Number of Nitrogen or Oxygen \leq 10; Number of NH or OH \leq 5), additionally, TPSA value ($<$ 140 Å²) (Table 2). Thus, we considered all 43 chemical constituents as drug-like compounds (DLCs).

Identifying of overlapping targets between SEA and STP databases

The targets related to DLCs were retrieved by SEA and STP databases, suggesting that targets recognized from SEA (423), and STP (444), respectively (**Supplementary Table S1**). The Venn diagram exhibited the overlapping targets (77) as significant targets of DLCs (**Supplementary Table S1**) (**Figure 3A**).

Recognition of obesity-related targets and final overlapping targets of AC on obesity

A total of 3,028 targets responded to occurrence and development of obesity were identified by DisGeNET and OMIM databases. Then, the Venn diagram showed that a total of 40 targets were overlapped between obesity-associated targets (3,028) and overlapped 77 targets (**Supplementary Table S2**) (**Figure 3B**).

The protein-protein-interaction (PPI) networks and topological analysis

The PPI networks were conducted to identify the uppermost target via RPackage, indicating that IL6 was the highest degree value (DV) among 40 targets. The 9 (ADH1B, CA3, SLC22A2, HSD11B2, OXER1, GSTK1, ENPP2, PAM, and SLC22A6) out of final 40 targets were removed due to no correlations each other, consisting of 31 nodes and 74 edges (**Figure 4**). In topological analysis, we performed analysis of degree centrality (DC) and betweenness centrality (BC) to identify an important target. The topological-based analysis was revealed that the IL6 was the highest DC (10) and BC (1) among 31 targets (**Table 3**). Thus, we considered the IL6 as a core target.

A hub pathway of AC against obesity

The Kyoto Encyclopedia of Genes and Genomes (KEGG) pathway analysis suggested that a total of 40 targets were associated with 2 pathways: (1) PPAR signaling pathway, (2) Insulin resistance against obesity. Based on the PPI network and topological analysis, we identified a hub pathway (Insulin resistance) correlated with IL6, in contrast, PPAR signaling pathway was no associated with IL6. The targets of the two pathways were exhibited in **Table 4**. In addition, a bubble graph indicated that insulin resistance is inactivated by DLCs of AC to alleviate obesity, due to lower rich factor than PPAR signaling pathway (**Figure 5**).

The analysis of pathways-targets-compounds (PTC) networks

A pathway-target-compound (PTC) network was constructed in **Figure 6**. The integrated network consisted of 30 nodes 61 edges. The nodes indicate a total number of each element: pathways, targets, and compounds. The edges stand for the associations of the three elements. The PTC network suggested that the 2 pathways, 7 targets, and 21 compounds are the significant factors to dampen obesity.

The molecular docking test (MDT) on a key target

The MDT was unveiled that IL6 (PDB ID: 4NI9) was related to 3 compounds out of DLCs from AC: (1) Andrographolide (PubChem ID: 5318517), (2) Deoxy-d-mannoic lactone (PubChem ID: 541561), and (3) Linoleic acid (PubChem ID: 5280450).

It was observed that Andrographolide (PubChem ID: 5318517) can dock as the most stable complex on IL6 (PDB ID: 4NI9), with -8.1 kcal/mol. Next, the binding energy of Deoxy-d-mannoic lactone (PubChem ID: 541561) was -6.3 kcal/mol with valid affinity (<-6.0 kcal/mol) [17]. Lastly, the affinity of Linoleic acid (PubChem ID: 5280450) was -5.0 kcal/mol with invalid binding energy. Noticeably, Andrographolide (PubChem ID: 5318517) can be considered as a potential IL6 inhibitor, compared with known 7 positive controls in aspects of binding energy (**Figure 7**), (**Table 5**).

Discussion

AC is a known as herbal plant to alleviate obesity, however, its chemical constituents are not elucidated completely, including potential targets, and effector pathways. In this study, we adopted GC-MS analysis to identify physicochemical properties such as lipophilicity and permeability [18]. Moreover, the profiled chemical constituents of GC-MS-based herbal plant metabolomics are based on a reliable reference database concerning bioavailability [19,20]. The target metabolites were analyzed by two cheminformatics: SEA was developed by Dr Shoichet's group to identify the interaction of between ligand(s) and target(s) as well as its relationships [21]; STP is an web-based online platform to be developed by SIB (Swiss Institute of Bioinformatics), which constructed 376,342 experimentally confirmed compounds and 3,068 targets since 2014 [22]. The final identified targets were analyzed by obesity-related targets, subsequently, we performed the PPI to identify the most significant target. On topological analysis, IL6 had the highest degree value (DV), degree centrality (DC), and betweenness centrality (BC). The DV is the number edges of targets [23]; DC is the net sum of total target connections [24]; and BC is the frequency with the shortest routes between each node [25]. In PPI networks, targets with high DC or BC are commonly the ones that give crucial hints to apply for therapeutic utilization relative significance of the targets in the integrated network analysis [26]. Then, we identified the IL6 with the highest DV, DC, and BC as a key target of AC on obesity. A report demonstrated that IL6 inhibitors have effects on reverse of body weight gain and body mass index (BMI) [27,28]. It implies that dampening of IL6 might be a promising future therapeutic strategy against obesity. The related pathways of AC on obesity were insulin resistance, and PPAR signaling pathway.

Only insulin resistance mechanism is directly related to the IL6, we then considered it as a key pathway. According to the bubble chart based on gene ratio, insulin resistance had lower rich factor than PPAR signaling pathway. It might thus be speculated that inactivation of insulin resistance could alleviate the progression of obesity. On MDT, there was an observational result that Andrographolide (PubChem ID: 5318517) with the highest affinity on IL6 is a potent effector against obesity. In particular, a study introduced that Andrographolide (PubChem ID: 5318517) or its derivatives have diverse biological activities, including obesity, hypertension, diabetes, and hyperlipidemia [29]. The Andrographolide (PubChem ID: 5318517) has noticeable efficacy on diminishing the glucose level in blood serum, and increasing in insulin in animal experiments [30]. The studies line up with our result. The PTC networks represent that treatment effect of AC on obesity was related directly to 2 pathways, 7 targets, and 21 chemical constituents. The KEGG pathway enrichment analysis

provides that Insulin resistance pathway and PPAR signaling pathway are associated with the development of obesity, indicating that the 2 pathways might be modulators to ameliorate obesity. Besides, Andrographolide (PubChem ID: 5318517) could bind more stably to IL6 than any other 7 positive controls (Gardenoside, 4-Methylesculetin, Auraptene, AX-024 HCl, APX-115 free base, Resatorvid, and Myrislignan). Thus, this study revealed a hub signaling pathway, a key target, and a key compound of AC against obesity, providing a therapeutic basis for further experimental verification.

Conclusions

To sum things up, this study provides the potential AC effector pathway to relieve obesity on a network pharmacology viewpoint. We elucidated that Andrographolide played a potent inhibitor on obesity by dampening IL6 on blocking insulin resistance. Besides, the MDT also verified that Andrographolide could form more stable complex with IL6, in comparison with 7 positive controls. However, in experimental aspects, this study has some limitations as clinical trial still is required to confirm our findings.

Materials And Methods

Plant material collection and extraction

Aralia cordata (AC) were obtained from (latitude: 35.993797, longitude: 128.768144) Gyeongsangbuk-do, Korea, in April 2021. The AC were dried in a shaded area with air ventilator at room temperature (20 ~ 22°C) for 2 weeks, and the dried AC pulverized with electric blender. Around 50g of AC powder was contained in 1L methyl alcohol (Daejung, Siheung city, Gyeonggi-do, Korea) for 10 days and repeated twice to acquire higher extraction amount. The solvent extract was collected, filtered with Whatman filter paper No. 1 (Whatman, Model no. WF1-1850, UK Maidstone) and evaporated utilizing a vacuum evaporator (IKA- RV8, Staufen city, Germany) at 40°C. The extraction amount after evaporating was 5.56 g (yield rate: 11.12%), which was calculated as follows.

Yield rate (%) = (Dried AC weight/Evaporated extraction weight) × 100

The conditions for GC-MS analysis

We utilized Agilent 7890A (Agilent, Santa Clara, CA, USA) to perform for GC-MS, its column was chosen as DB-5 (30 m × 0.25 mm × 0.25 μm) (Agilent, Santa Clara, CA, USA) with nonpolar properties. The GC-MS was maintained at 100 °C for 2.1 min, which increased gradually to 300 °C at a rate of 25 °C/min and was steady for 20 min. Injection port temperature and helium flow rate were set up as 250 °C and 1.5 mL/min, respectively. The ionization voltage was 70 eV. The split mode of sample injection was at 10:1 and the Mass Spectra (MS) detection range consisted of 35–900 (m/z). The fragmentation modes of MS were compared with the W8N05ST Library MS database (analyzed 13 July 2021). The ratio of each compound was determined from the relative integral value of each compound in the chromatogram [31].

Identifying of chemical composition in AC and screening of drug-like compounds

The chemical compositions in AC were identified through GC-MS analysis, which were converted into Simplified Molecular Input Line Entry System (SMILES) format via PubChem (<https://pubchem.ncbi.nlm.nih.gov/>) (accessed on 19 July 2021). Then, we adopted Lipinski's rule to screen drug-like compounds (DLCs) via SwissADME (<http://www.swissadme.ch/>) (accessed on 19 July 2021). Additionally, we considered the topological polar surface area to facilitate cell permeability, its standard threshold value is less than 140 Å² [32].

Targets related to DLCs from AC or obesity

The targets associated with DLCs were retrieved by public cheminformatics: Similarity Ensemble Approach (SEA) (accessed on 22 July 2021) [33], SwissTargetPrediction (STP) (accessed on 22 July 2021) [34] on "*Homo Sapiens*" module. The association between targets and DLCs were identified by the two databases, which established their utilization as important tools to be verified in experiment: Around 80% out of drug candidates match up the SEA information, also, the potential targets of Cudraflavone C were selected by STP, thereby, its bioactivities were verified by experiment [35,36]. In parallel, the targets connected with DLCs were retrieved by DisGeNET (<https://www.disgenet.org/>) (accessed on 23th July 2021) and OMIM (<https://www.omim.org/>) (accessed on 23th July 2021). The final overlapping targets between collected DLCs-related targets and obesity-associated targets were confirmed and visualized by Venn diagram plotter.

The protein-protein interaction (PPI) networks construction and topological analysis

The final overlapping targets were constructed PPI networks to analyze the uppermost target among targets. The most significant considerable elements are Degree Value (DV; edges number of targets) [23], Degree Centrality (DC; the total number of target connection) [37], and Betweenness Centrality (BC; the number of targets as the shortest route between two other targets) [38]. Then, we identified the most noticeable target in PPI networks.

Identifying of two pathways related to occurrence and development of obesity

We constructed a bubble chart based on gene ratio, thereby, suggested crucial two pathways associated with AC on obesity. Particularly, the pathway consisted of a key target (the highest DV, DC, and BC) was defined as a hub pathway of AC on obesity.

The analysis of integrated pathways-targets-compounds (PTC) networks

The PTC networks were constructed as a size map, based on DV. In the integrated networks, taking AC, pathways, targets, and compounds as nodes, its relationships were indicated as edges. The yellow rectangles (nodes) signified the pathway(s); the blue triangles (nodes) represented the target(s); and the red violet stood for the compound(s). Then, the gray line represented the corresponding relationship. The merged PTC networks were plotted by RPackage.

The preparation for molecular docking test (MDT)

We prepared for the MDT between a hub pathway and ligands. The key target related to a hub pathway was identified by RCSB PDB (<https://www.rcsb.org/>) (accessed on 27th July 2021). The .pdb format was converted into .pdbqt format via Autodock tool (<https://autodock.scripps.edu/>) (accessed on 28th July 2021) in order to conduct the MDT. Then, the DLCs associated with the key target were identified .sdf format by PubChem, sequentially, the .sdf format was converted into .pdb format via Pymol.

MDT of compounds on targets associated with a key pathway

The compounds and targets related to a key pathway were docked utilizing autodock4 by setting-up 4 energy range and 8 exhaustiveness to identify 10 different complexes [39]. The center of a key target on the key pathway was IL6 ($x = 11.213$, $y = 33.474$, $z = 11.162$). The active site's cube box was $x = 40 \text{ \AA}$, $y = 40 \text{ \AA}$, $z = 40 \text{ \AA}$. The interaction of 2D binding was illustrated by LigPlot⁺ 2.2 (<https://www.ebi.ac.uk/thornton-srv/software/LigPlus/>) (accessed on 29th July 2021) [40].

Abbreviations

AC, *Aralia cordata*;

BC, Betweenness Centrality;

BMI, Body Mass Index;

DC, Degree Centrality;

DLCs, Drug-Like Compounds;

DV, Degree Value;

GC-MS, Gas Chromatography Mass Spectrum;

KEGG, Kyoto Encyclopedia of Genes and Genomes;

MDT, Molecular Docking Test;

PPI, Protein-Protein Interaction;

PTC, Pathways-Targets-Compounds;

SEA, Similarity Ensemble Approach;

SIB, Swiss Institute of Bioinformatics;

SMILES, Simplified Molecular Input Line Entry System;

STP, SwissTargetPrediction;

WHO, World Health Organization

Declarations

Data availability statement

All data generated or analyzed during this study are included in this published article (and its Supplementary Materials).

Acknowledgements

This research was acknowledged by the Department of Bio-Health Convergence, Kangwon National University, Chuncheon 24341, Republic of Korea.

Conflicts of interest

The authors have declared no conflict of interest. They have no known competing financial interests or personal relationships that could have appeared to influence the research reported in this publication.

References

1. Cercato, C.; Fonseca, F.A. Cardiovascular risk and obesity. *Diabetology and Metabolic Syndrome* **2019**, *11*, 1–15, doi:10.1186/S13098-019-0468-0/TABLES/1.
2. Obesity and overweight Available online: <https://www.who.int/news-room/fact-sheets/detail/obesity-and-overweight> (accessed on Jan 13, 2022).
3. Leeners, B.; Geary, N.; Tobler, P.N.; Asarian, L. Ovarian hormones and obesity. *Human Reproduction Update* **2017**, *23*, 300–321, doi:10.1093/HUMUPD/DMW045.

4. Klötting, N.; Fasshauer, M.; Dietrich, A.; Kovacs, P.; Schön, M.R.; Kern, M.; Stumvoll, M.; Blüher, M. Insulin-sensitive obesity. *American Journal of Physiology - Endocrinology and Metabolism* **2010**, *299*, 506–515, doi:10.1152/AJPENDO.00586.2009/SUPPL_FILE/SUPPMAT.PDF.
5. Flegal, K.M.; Carroll, D.; Kit, B.K.; Ogden, C.L. Prevalence of Obesity and Trends in the Distribution of Body Mass Index Among US Adults, 1999-2010. *JAMA* **2012**, *307*, 491–497, doi:10.1001/JAMA.2012.39.
6. Sahoo, K.; Sahoo, B.; Choudhury, A.K.; Sofi, N.Y.; Kumar, R.; Bhadoria, A.S. Childhood obesity: causes and consequences. *Journal of Family Medicine and Primary Care* **2015**, *4*, 187, doi:10.4103/2249-4863.154628.
7. Kim, G.W.; Lin, J.E.; Blomain, E.S.; Waldman, S.A. Anti-Obesity Pharmacotherapy: New Drugs and Emerging Targets. *Clinical pharmacology and therapeutics* **2014**, *95*, 53, doi:10.1038/CLPT.2013.204.
8. Tak, Y.J.; Lee, S.Y. Anti-Obesity Drugs: Long-Term Efficacy and Safety: An Updated Review. *The World Journal of Men's Health* **2021**, *39*, 208, doi:10.5534/WJMH.200010.
9. Coulter, A.A.; Rebello, C.J.; Greenway, F.L. Centrally Acting Drugs for Obesity: Past, Present, and Future. *Drugs* **2018**, *78*, 1113, doi:10.1007/S40265-018-0946-Y.
10. Wilding, J.P.H. Combination therapy for obesity. *Journal of psychopharmacology (Oxford, England)* **2017**, *31*, 1503–1508, doi:10.1177/0269881117737401.
11. Fan, Q.; Xu, F.; Liang, B.; Zou, X. The Anti-Obesity Effect of Traditional Chinese Medicine on Lipid Metabolism. *Frontiers in Pharmacology* **2021**, *12*, 1486, doi:10.3389/FPHAR.2021.696603/BIBTEX.
12. Ock Kim, M.; Hwa Lee, S.; Hee Seo, J.; Soon Kim, I.; Reum Han, A.; Oh Moon, D.; Cho, S.; Cui, L.; Kim, J.; Sun Lee, H. *Artemisia annua* Inhibits Triacylglycerol Biosynthesis in HepG2 Cells., doi:10.1089/jmf.2012.2636.
13. Chandran, U.; Mehendale, N.; Patil, S.; Chaguturu, R.; Patwardhan, B. Network Pharmacology. *Innovative Approaches in Drug Discovery* **2017**, *127*, doi:10.1016/B978-0-12-801814-9.00005-2.
14. Wang, Y.; Hu, B.; Feng, S.; Wang, J.; Zhang, F. Target recognition and network pharmacology for revealing anti-diabetes mechanisms of natural product. *Journal of Computational Science* **2020**, *45*, doi:10.1016/J.JOCS.2020.101186.
15. Zhao, F.; Guochun, L.; Yang, Y.; Shi, L.; Xu, L.; Yin, L. A network pharmacology approach to determine active ingredients and rationality of herb combinations of Modified-Simiaoan for treatment of gout. *Journal of Ethnopharmacology* **2015**, *168*, 1–16, doi:10.1016/J.JEP.2015.03.035.
16. Li, W.; Yuan, G.; Pan, Y.; Wang, C.; Chen, H. Network Pharmacology Studies on the Bioactive Compounds and Action Mechanisms of Natural Products for the Treatment of Diabetes Mellitus: A Review. *Frontiers in Pharmacology* **2017**, *8*, doi:10.3389/FPHAR.2017.00074.
17. Shityakov, S.; Förster, C. In silico predictive model to determine vector-mediated transport properties for the blood-brain barrier choline transporter. *Advances and applications in bioinformatics and chemistry: AABC* **2014**, *7*, 23–36, doi:10.2147/AABC.S63749.
18. Sympli, H.D. Estimation of drug-likeness properties of GC-MS separated bioactive compounds in rare medicinal *Pleione maculata* using molecular docking technique and SwissADME in silico tools. *Network Modeling and Analysis in Health Informatics and Bioinformatics* **2021**, *10*, doi:10.1007/S13721-020-00276-1.
19. Khan, W.; Parveen, R.; Chester, K.; Parveen, S.; Ahmad, S. Hypoglycemic Potential of Aqueous Extract of *Moringa oleifera* Leaf and In Vivo GC-MS Metabolomics. *Frontiers in pharmacology* **2017**, *8*, doi:10.3389/FPHAR.2017.00577.
20. Rodriguez-Cabezas, E.; Tenori, L.; Hafizur, M.; Ansari, R.; Khan, W.; Parveen, R.; Saher, S.; Ahmad, S. Pharmacokinetic, Metabolomic, and Stability Assessment of Ganoderic Acid H Based Triterpenoid Enriched Fraction of *Ganoderma lucidum* P. Karst. *Metabolites* **2022**, *Vol. 12*, Page 97 **2022**, *12*, 97, doi:10.3390/METABO12020097.
21. Keiser, M.J.; Setola, V.; Irwin, J.J.; Laggner, C.; Abbas, A.I.; Hufeisen, S.J.; Jensen, N.H.; Kuijer, M.B.; Matos, R.C.; Tran, T.B.; et al. Predicting new molecular targets for known drugs. *Nature* **2009**, *462*, 175–181, doi:10.1038/nature08506.
22. Daina, A.; Michielin, O.; Zoete, V. SwissTargetPrediction: updated data and new features for efficient prediction of protein targets of small molecules. *Nucleic Acids Research* **2019**, *47*, W357, doi:10.1093/NAR/GKZ382.
23. Jiang, Y.; Zhong, M.; Long, F.; Yang, R.; Zhang, Y.; Liu, T. Network pharmacology-based prediction of active ingredients and mechanisms of *lamiophlomis rotata* (Benth.) kudo against rheumatoid arthritis. *Frontiers in Pharmacology* **2019**, *10*, 1435, doi:10.3389/FPHAR.2019.01435/BIBTEX.
24. Harrold, J.M.; Ramanathan, M.; Mager, D.E. Network-Based Approaches in Drug Discovery and Early Development. *Clinical pharmacology and therapeutics* **2013**, *94*, 651, doi:10.1038/CLPT.2013.176.
25. Boezio, B.; Audouze, K.; Ducrot, P.; Taboureau, O. Network-based Approaches in Pharmacology. *Molecular Informatics* **2017**, *36*, 1700048, doi:10.1002/MINF.201700048.
26. Somolinos, F.J.; León, C.; Guerrero-Aspizua, S. Drug Repurposing Using Biological Networks. *Processes* **2021**, *Vol. 9*, Page 1057 **2021**, *9*, 1057, doi:10.3390/PR9061057.
27. Patsalos, O.; Dalton, B.; Himmerich, H. Effects of IL-6 Signaling Pathway Inhibition on Weight and BMI: A Systematic Review and Meta-Analysis. *International journal of molecular sciences* **2020**, *21*, 1–13, doi:10.3390/IJMS21176290.
28. Ma, Y.; Gao, M.; Sun, H.; Liu, D. Interleukin-6 gene transfer reverses body weight gain and fatty liver in obese mice. *Biochimica et Biophysica Acta (BBA) - Molecular Basis of Disease* **2015**, *1852*, 1001–1011, doi:10.1016/J.BBADDIS.2015.01.017.
29. Islam, M.T. Andrographolide, a New Hope in the Prevention and Treatment of Metabolic Syndrome. *Frontiers in Pharmacology* **2017**, *8*, doi:10.3389/FPHAR.2017.00571.
30. Thakur, A.K.; Rai, G.; Chatterjee, S.S.; Kumar, V. Beneficial effects of an *Andrographis paniculata* extract and andrographolide on cognitive functions in streptozotocin-induced diabetic rats. *Pharmaceutical biology* **2016**, *54*, 1528–1538, doi:10.3109/13880209.2015.1107107.

31. Oh, K.K.; Adnan, M.; Cho, D.H. A network pharmacology analysis on drug-like compounds from *Ganoderma lucidum* for alleviation of atherosclerosis. *Journal of Food Biochemistry* **2021**, *45*, e13906, doi:10.1111/JFBC.13906.
32. Matsson, P.; Kihlberg, J. How Big Is Too Big for Cell Permeability? *Journal of Medicinal Chemistry* **2017**, *60*, 1662–1664, doi:10.1021/ACS.JMEDCHEM.7B00237.
33. Keiser, M.J.; Roth, B.L.; Armbruster, B.N.; Emsberger, P.; Irwin, J.J.; Shoichet, B.K. Relating protein pharmacology by ligand chemistry. *Nature Biotechnology* **2007**, *25*, 197–206, doi:10.1038/nbt1284.
34. Daina, A.; Michielin, O.; Zoete, V. SwissTargetPrediction: updated data and new features for efficient prediction of protein targets of small molecules. *Nucleic Acids Research* **2019**, *47*, W357–W3664, doi:10.1093/NAR/GKZ382.
35. Singh, N.; Chaput, L.; Villoutreix, B.O. Virtual screening web servers: designing chemical probes and drug candidates in the cyberspace. *Briefings in Bioinformatics* **2021**, *22*, 1790–1818, doi:10.1093/BIB/BBAA034.
36. Soo, H.C.; Chung, F.F.L.; Lim, K.H.; Yap, V.A.; Bradshaw, T.D.; Hii, L.W.; Tan, S.H.; See, S.J.; Tan, Y.F.; Leong, C.O.; et al. Cudraflavone C Induces Tumor-Specific Apoptosis in Colorectal Cancer Cells through Inhibition of the Phosphoinositide 3-Kinase (PI3K)-AKT Pathway. *PLOS ONE* **2017**, *12*, e0170551, doi:10.1371/JOURNAL.PONE.0170551.
37. Zeng, Q.; Li, L.; Siu, W.; Jin, Y.; Cao, M.; Li, W.; Chen, J.; Cong, W.; Ma, M.; Chen, K.; et al. A combined molecular biology and network pharmacology approach to investigate the multi-target mechanisms of Chaihu Shugan San on Alzheimer's disease. *Biomedicine & Pharmacotherapy* **2019**, *120*, 109370, doi:10.1016/J.BIOPHA.2019.109370.
38. Zhang, L.; Shi, X.; Huang, Z.; Mao, J.; Mei, W.; Ding, L.; Zhang, L.; Xing, R.; Wang, P. Network Pharmacology Approach to Uncover the Mechanism Governing the Effect of *Radix Achyranthis Bidentatae* on Osteoarthritis. *BMC Complementary Medicine and Therapies* **2020**, *20*, doi:10.1186/S12906-020-02909-4.
39. Khanal, P.; Patil, B.M.; Chand, J.; Naaz, Y. Anthraquinone Derivatives as an Immune Booster and their Therapeutic Option Against COVID-19. *Natural Products and Bioprospecting* **2020**, *10*, 325–335, doi:10.1007/S13659-020-00260-2/FIGURES/4.
40. Laskowski, R.A.; Swindells, M.B. LigPlot+: Multiple Ligand–Protein Interaction Diagrams for Drug Discovery. *Journal of Chemical Information and Modeling* **2011**, *51*, 2778–2786, doi:10.1021/CI200227U.

Tables

Table 1. A list of identified 43 chemical compounds from AC via GC-MS.

No.	Compounds	PubChem ID	RT (mins)	Area (%)	Taxonomic compound classification
1	Cyclopentanone dimethylhydrazone	277539	3.654	1.00	Organonitrogen compounds
2	Dodecylamine	13583	3.818	0.30	Organonitrogen compounds
3	4H-Pyran-4-one, 2,3-dihydro-3,5-dihydroxy-6-methyl-	119838	4.048, 4.106, 4.366	2.03	Pyrans
4	Erythritol	222285	4.481	0.12	Organooxygen compounds
5	5-Hydroxymethylfurfural	237332	4.808, 5.327	8.83	Organooxygen compounds
6	2-Butenal, 2-methyl-, dimethylhydrazone	9601577	5.616	0.08	Organonitrogen compounds
7	Octanal	454	5.693	0.09	Organooxygen compounds
8	γ -Elemene	6432312	5.818	0.32	Prenol lipids
9	Butanamide, N-propyl-	231083	6.01	0.06	Prenol lipids
10	trans- α -Bergamotene	6429302	6.087	0.22	Prenol lipids
11	Germacrene D	5373727	6.144	0.10	Prenol lipids
12	1,4-Dideuteriooctane	151945284	6.231	0.17	Pyridines and derivatives
13	Tetradecylamine	16217	6.481	1.51	Organonitrogen compounds
14	Octanoic acid	379	6.625	0.24	Fatty Acyls
15	7-Methyl-3,4,5,6,7,8-hexahydronaphthalen-1(2h)-one	12259411	6.721	0.22	Organooxygen compounds
16	Calarene	28481	6.885	0.05	Prenol lipids
17	2-Carbamyl-9-[β -d-ribofuranosyl]hypoxanthine	14191026	7.048	0.08	Purine nucleosides
18	Decanoic acid	2969	7.202	0.32	Fatty Acyls
19	1,3,4,5-Tetrahydroxycyclohexanecarboxylic acid	1064	7.269	0.46	Organooxygen compounds
20	1-Deoxy-d-altritol	18667263	7.308	0.18	Organooxygen compounds
21	3-Deoxy-d-mannoic lactone	541561	7.366, 7.404	0.50	Lactones
22	Tonalid	89440	7.991	0.13	Tetralins
23	Methyl palmitate	8181	8.048	0.23	Fatty Acyls
24	2-(pentafluorophenoxy)acetamide	262900	8.116	0.07	Phenol ethers
25	13-Apo- β -carotenone	5363697	8.164	0.06	Prenol lipids
26	Palmitic acid	985	8.25	0.52	Fatty Acyls
27	Longifolene	289151	8.298	0.35	Prenol lipids
28	Falcarinol	5281149	8.548	0.16	Fatty Acyls
29	Linoleic acid	5280450	8.721	0.54	Fatty Acyls
30	4-Camphenylbutan-2-one	540428	8.856	0.37	Prenol lipids
31	Dextropimarinal	12304198	9.173	7.03	Prenol lipids
32	2-tert-Butyltetralin	142566	9.231	0.35	Tetralins
33	Naphthalen-1,4-imine,1,4-dihydro-9-methyl-	143264	9.289	2.43	Naphthalenes
34	1-Naphthalenepropanol, α -ethenyldecahydro-5-(hydroxymethyl)- α ,2,5,5,8a-pentamethyl-	543439	9.336	0.22	Prenol lipids
35	Vulgarol A	91746444	9.471	2.16	Prenol lipids
36	7-Phenyl-9H-indeno[2,1-C]pyridin-9-one	71386832	9.519	2.43	Organooxygen compounds
37	Bicyclo[5.2.0]nonane, 4-methylene-2,8,8-trimethyl-2-vinyl-	557143	9.587	2.61	Unsaturated

					hydrocarbons
38	4-Aminobutyramide, N-methyl-N-[4-(1-pyrrolidiny)-2-butynyl]-	578315	9.846	15.92	Carboxylic acids and derivatives
39	8-Methylenedispiro[2.1.2.4]undecane	561669	9.894	12.07	Unsaturated hydrocarbons
40	Andrographolide	5318517	10.01	3.24	Lactones
41	Kaurenoic acid	73062	10.068, 10.106, 10.279, 10.798, 11.135	28.48	Prenol lipids
42	Stigmasterol	5280794	14.135	0.23	Steroids and steroid derivatives
43	Clionasterol	457801	14.702	0.32	Steroids and steroid derivatives

Table 2. A profiling of physicochemical properties of 43 chemical compounds.

No.	Compounds	Lipinski Rules				Lipinski's Violations	Bioavailability Score	TPSA(Å²)
		MW	HBA	HBD	MLog P			
		< 500	< 10	≤ 5	≤ 4.15			
1	Cyclopentanone dimethylhydrazone	126.20	1	0	1.23	0	0.55	15.60
2	Dodecylamine	185.35	1	1	3.41	0	0.55	26.02
3	4H-Pyran-4-one, 2,3-dihydro-3,5-dihydroxy-6-methyl-	144.13	4	2	-1.77	0	0.85	66.76
4	Erythritol	122.12	4	4	-1.91	0	0.55	80.92
5	5-Hydroxymethylfurfural	126.11	3	1	-1.06	0	0.55	50.44
6	2-Butenal, 2-methyl-, dimethylhydrazone	126.20	1	0	1.52	0	0.55	15.60
7	Octanal	128.21	1	0	2.07	0	0.55	17.07
8	γ-Elemene	204.35	0	0	4.53	1	0.55	0.00
9	Butanamide, N-propyl-	129.20	1	1	1.22	0	0.55	29.10
10	trans-α-Bergamotene	204.35	0	0	4.63	1	0.55	0.00
11	Germacrene D	204.35	0	0	4.53	1	0.55	0.00
12	1,4-Dideuteriooctane	114.23	0	0	4.20	1	0.55	0.00
13	Tetradecylamine	213.40	1	1	3.95	0	0.55	26.02
14	Octanoic acid	144.21	2	1	1.96	0	0.85	37.30
15	7-Methyl-3,4,5,6,7,8-hexahydronaphthalen-1(2h)-one	164.24	1	0	2.49	0	0.55	17.07
16	Calarene	204.35	0	0	5.65	1	0.55	0.00
17	2-Carbamyl-9-[β-d-ribofuranosyl]hypoxanthine	295.25	8	4	-3.28	0	0.55	156.61
18	Decanoic acid	172.26	2	1	2.58	0	0.85	37.30
19	1,3,4,5-Tetrahydrocyclohexanecarboxylic acid	192.17	6	5	-2.14	0	0.55	118.22
20	1-Deoxy-d-altritol	166.17	5	5	-1.95	0	0.55	101.15
21	3-Deoxy-d-mannoic lactone	162.14	5	3	-1.68	0	0.55	86.99
22	Tonalid	258.40	1	0	4.10	0	0.55	17.07
23	Methyl palmitate	270.45	2	0	4.44	1	0.55	26.30
24	2-(pentafluorophenoxy)acetamide	241.11	7	1	2.75	0	0.55	52.32
25	13-Apo-β-carotenone	258.40	1	0	4.02	0	0.55	17.07
26	Palmitic acid	256.42	2	1	4.19	1	0.85	37.30
27	Longifolene	204.35	0	0	5.65	1	0.55	5.65
28	Falcarinol	244.37	1	1	4.26	1	0.55	20.23
29	Linoleic acid	280.45	2	1	4.47	1	0.85	37.30
30	4-Camphenylbutan-2-one	206.32	1	0	3.30	0	0.55	17.07
31	Dextropimarinal	286.45	1	0	4.65	1	0.55	17.07
32	2-tert-Butyltetralin	188.31	0	0	5.19	1	0.55	0.00
33	Naphthalen-1,4-imine,1,4-dihydro-9-methyl-	157.21	1	0	2.30	0	0.55	3.24
34	1-Naphthalenepropanol, α-ethenyldecahydro-5-(hydroxymethyl)-α,2,5,5,8a-pentamethyl-	308.50	2	2	3.93	0	0.55	40.46
35	Vulgarol A	308.50	2	2	3.93	0	0.55	40.46
36	7-Phenyl-9H-indeno[2,1-C]pyridin-9-one	257.29	2	0	2.7	0	0.55	29.96
37	Bicyclo[5.2.0]nonane, 4-methylene-2,8,8-trimethyl-2-vinyl-	204.35	0	0	4.63	1	0.55	0.00
38	4-Aminobutyramide, N-methyl-N-[4-(1-pyrrolidinyl)-2-butyryl]-	237.34	3	1	0.79	0	0.55	49.57
39	8-Methylenedispiro[2.1.2.4]undecane	162.27	0	0	4.86	1	0.55	0.00

40	Andrographolide	350.45	5	3	1.98	0	0.55	86.99
41	Kaurenoic acid	302.45	2	1	4.63	1	0.85	37.30
42	Stigmasterol	412.69	1	1	6.62	1	0.55	20.23
43	Clonasterol	414.71	1	1	6.73	1	0.55	20.23

Table 3. The topological analysis of PPI networks.

No.	Target	Degree of value (DV)	Degree of centrality (DC)	Betweenness centrality (BC)
1	IL6	18	10	1.00
2	PPARG	12	3	0.28
3	MGLL	8	4	0.23
4	HNF4A	5	3	0.17
5	CES1	3	2	0.12
6	KAT2B	4	1	0.05
7	PPARA	10	1	0.03
8	ESR1	9	9	0.00
9	CNR1	7	7	0.00
10	FABP4	7	7	0.00
11	FFAR4	4	4	0.00
12	NR1H2	4	4	0.00
13	CNR2	4	3	0.00
14	ESR2	4	3	0.00
15	NR1H3	6	3	0.00
16	G6PD	2	2	0.00
17	GLI1	3	2	0.00
18	NAAA	4	2	0.00
19	ADA	1	1	0.00
20	CA5A	1	1	0.00
21	EHMT1	1	1	0.00
22	NR4A1	2	1	0.00
23	CES2	1	0	0.00
24	TRPV1	7	0	0.00
25	PDCD4	1	0	0.00
26	SHBG	3	0	0.00
27	PTPRC	5	0	0.00
28	NR1H4	4	0	0.00
29	PPARD	4	0	0.00
30	VDR	3	0	0.00
31	THRB	1	0	0.00

Table 4. Targets in 2 pathways related to obesity.

KEGG ID & Description	Targets	False discovery rate
hsa04370: Insulin resistance	NR1H2, IL6, NR1H3, PPARA	0.00027
hsa03320: PPAR signaling pathway	NR1H3, FABP4, PPARG, PPARD	0.00710

Table 5. Binding energy and interactions of chemical compounds on IL6 and positive controls.

Protein	Ligand	PubChem ID	Compound classification	Binding energy(kcal/mol)	Grid box		Hydrogen Bond Interactions	Hydrophobic Interactions
					Center	Dimension	Amino acid Residue	Amino acid Res
IL6 (PDB ID: 4NI9)	Andrographolide	5318517	Lactones	-8.1	x=11.213	size_x = 40	N/A	Glu110, Gln111, Ala114
					y=33.474	size_y = 40		
					z=11.162	size_z = 40		
	3-Deoxy-d-mannoic lactone	541561	Lactones	-6.3	x=11.213	size_x = 40	N/A	N/A
					y=33.474	size_y = 40		
					z=11.162	size_z = 40		
	Linoleic acid	5280450	Fatty acyls	-5.0	x=11.213	size_x = 40	N/A	Pro80, Glu81, S
					y=33.474	size_y = 40		
					z=11.162	size_z = 40		
Positive control	Gardenoside	24721095	Iridoid O-glycosides	-7.8	x=11.213	size_x = 40	Tyr31, Asp34, Gln111	N/A
					y=33.474	size_y = 40		
					z=11.162	size_z = 40		
	4-Methylesculetin	5319502	6,7-dihydroxycoumarins	-7.6	x=11.213	size_x = 40	Arg24, Arg16	Pro18
					y=33.474	size_y = 40		
					z=11.162	size_z = 40		
	Auraptene	1550607	Terpene lactones	-7.6	x=11.213	size_x = 40	N/A	Asp34, Glu110, Tyr31
					y=33.474	size_y = 40		
					z=11.162	size_z = 40		
AX-024 HCl	129909862	Neoflavones	-7.5	x=11.213	size_x = 40	N/A	Gln111, Tyr31, Asp34	
				y=33.474	size_y = 40			
				z=11.162	size_z = 40			
APX-115 free base	51036475	Pyrazolopyridines	-7.2	x=11.213	size_x = 40	Tyr31	Glu110, Gln111, Asp34	
				y=33.474	size_y = 40			
				z=11.162	size_z = 40			
Resatorvid	11703255	Sulfanilides	-7.1	x=11.213	size_x = 40	Tyr31, Gln111	Glu110, Asp34	
				y=33.474	size_y = 40			
				z=11.162	size_z = 40			
Myrislignan	21636106	Lignans, neolignans and related compounds	-7.1	x=11.213	size_x = 40	Gln111	Tyr31, Gly35, Asp34	
				y=33.474	size_y = 40			
				z=11.162	size_z = 40			

Figures

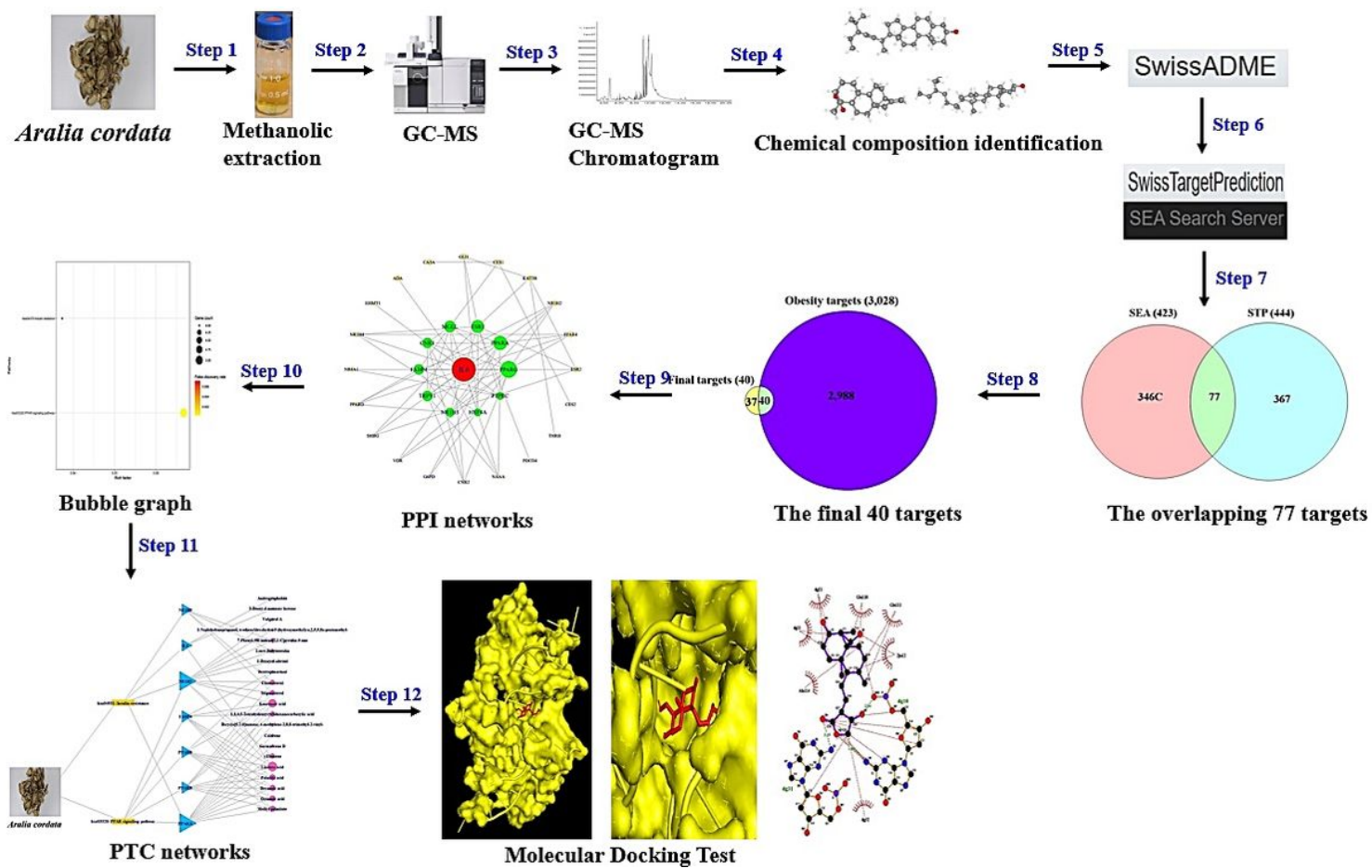


Figure 1

The workflow of this study on network pharmacology.

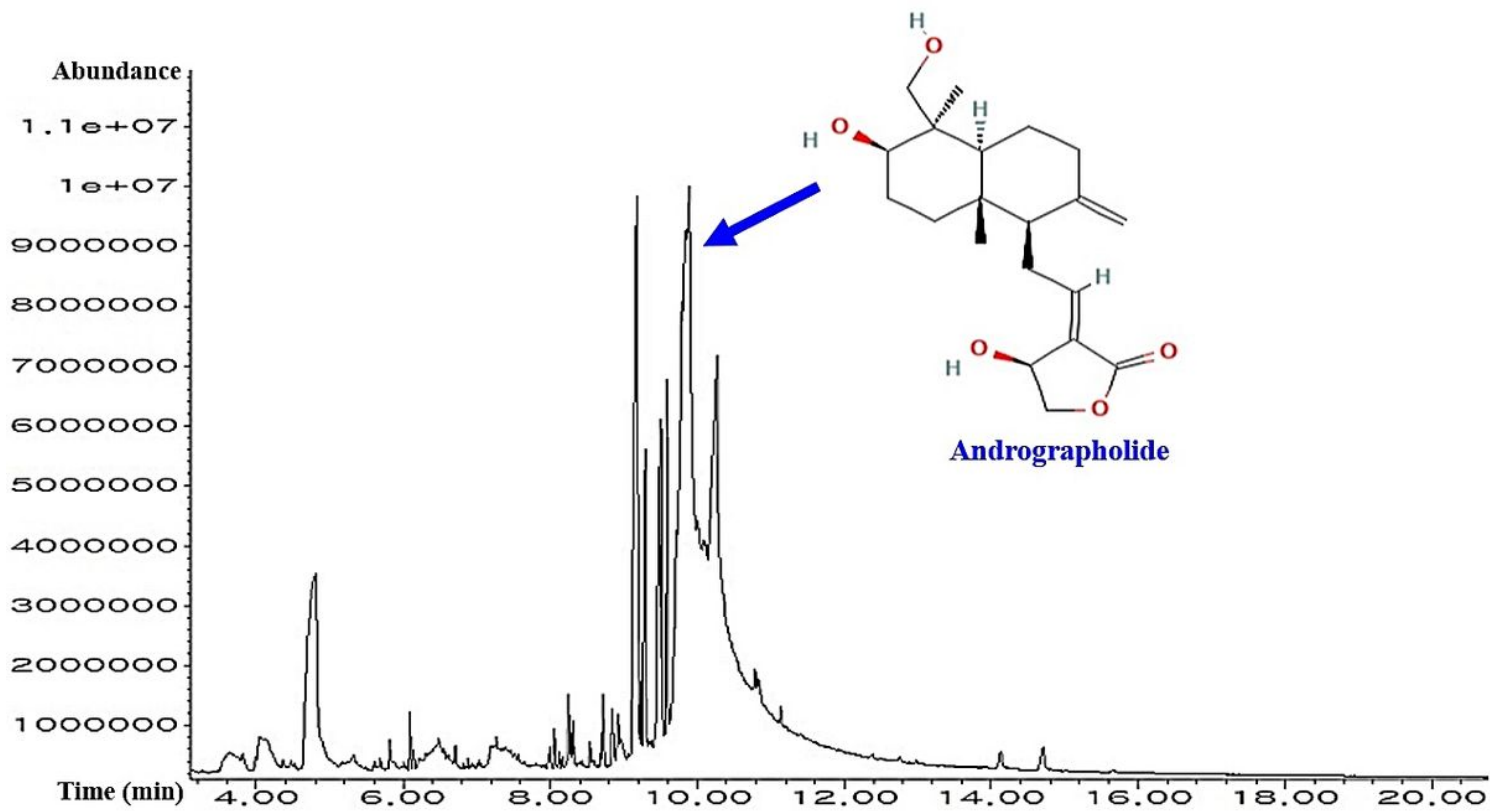
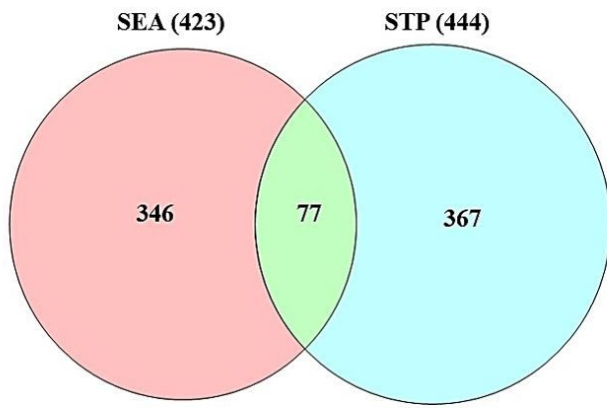


Figure 2

The GC chromatograms and a key compound of AC.

(A)



(B)

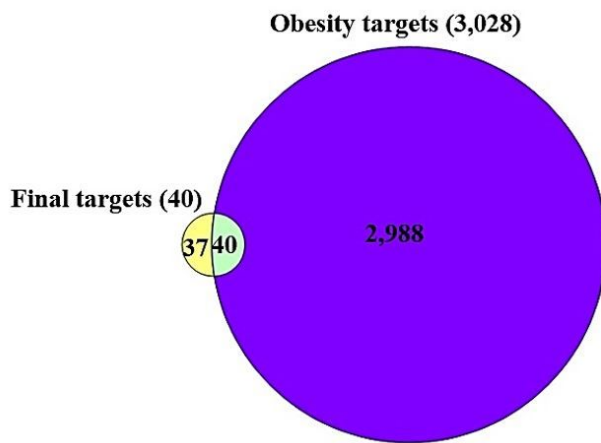


Figure 3

- (a) The overlapping targets (77) between SEA (423) and STP (444) databases.
- (b) The final targets (40) between the overlapping targets (77) and obesity-related targets (3,028).

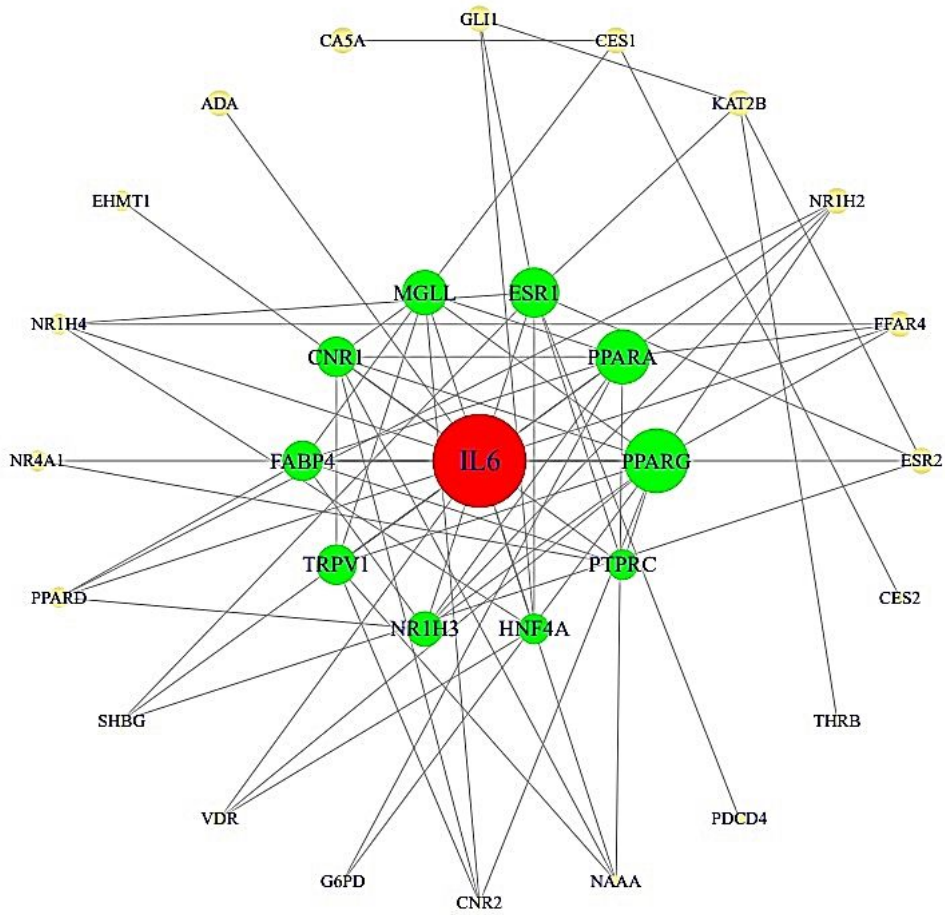


Figure 4

PPI networks (31 nodes, 74 edges).

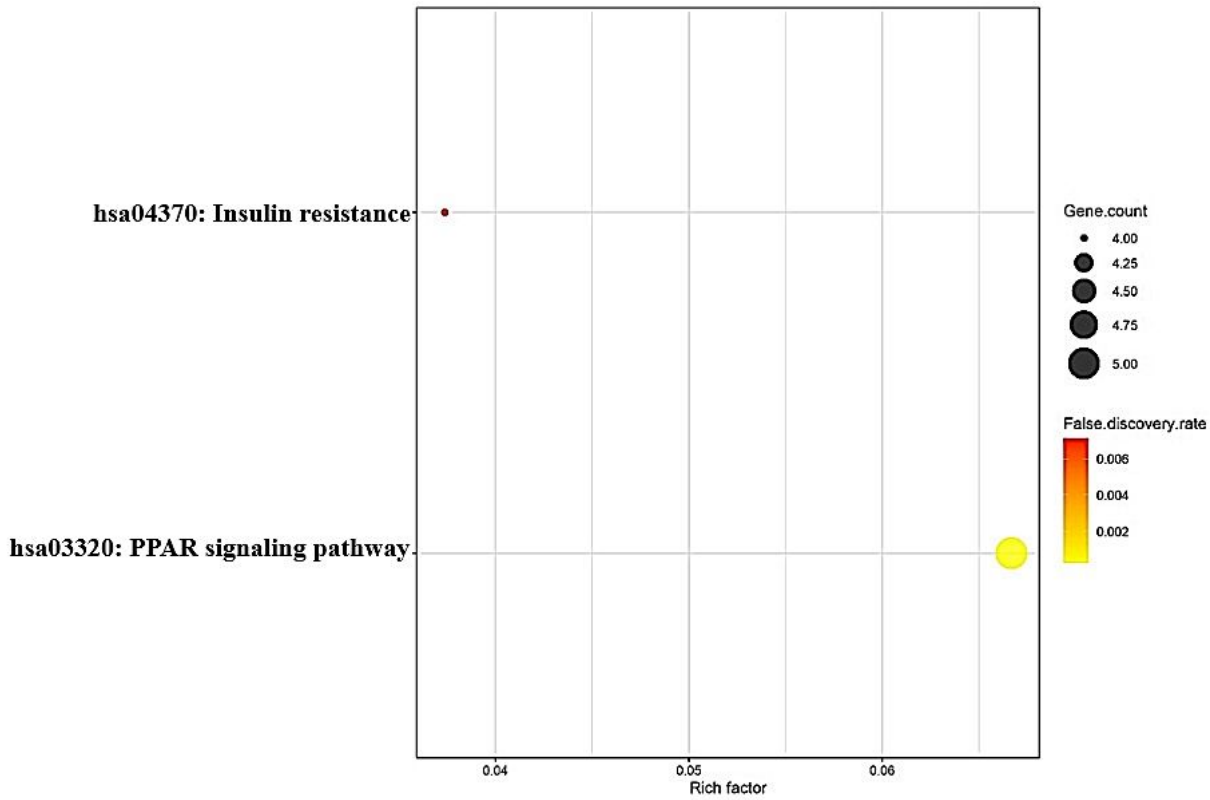


Figure 5

A bubble chart associated with obesity.

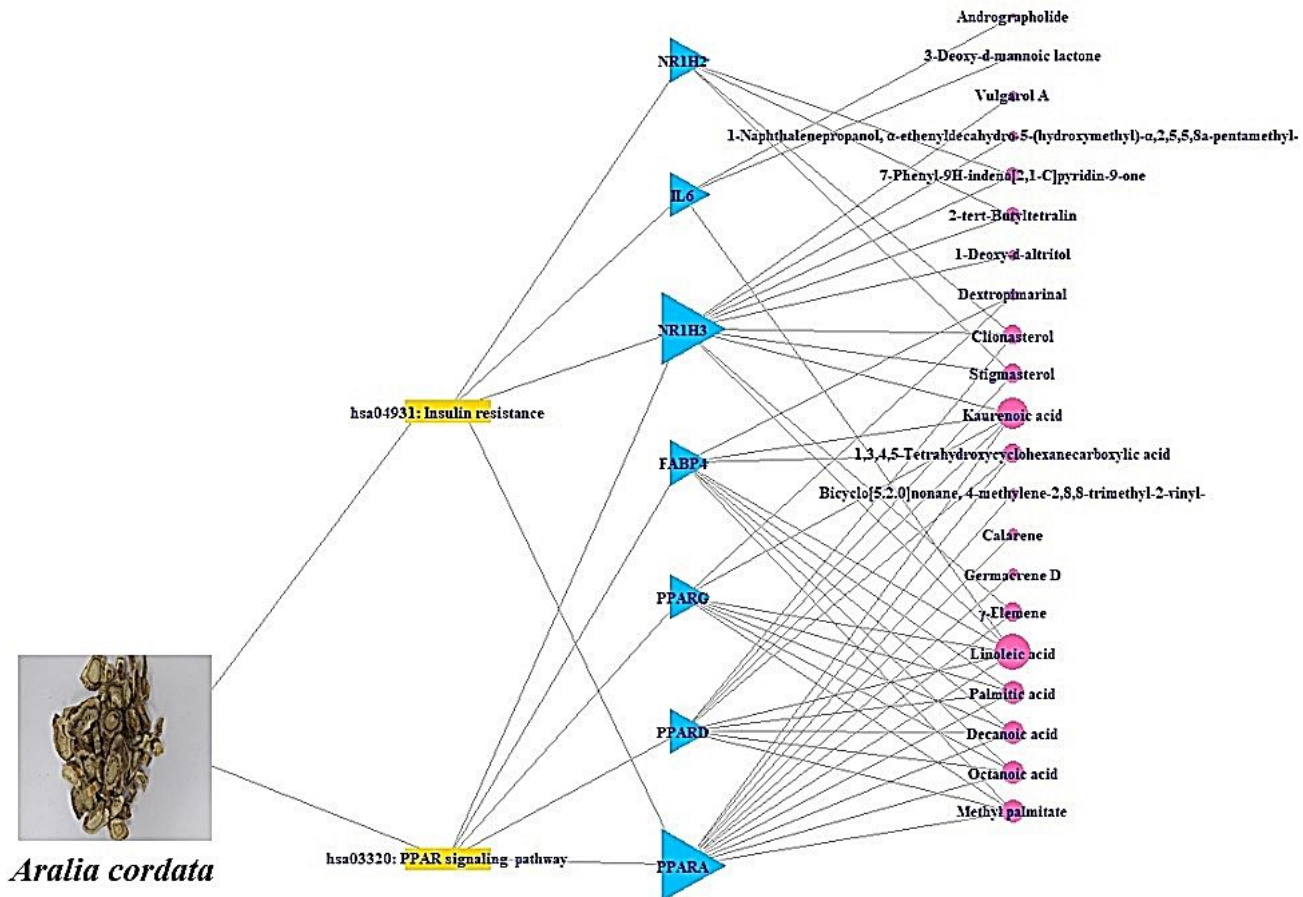


Figure 6

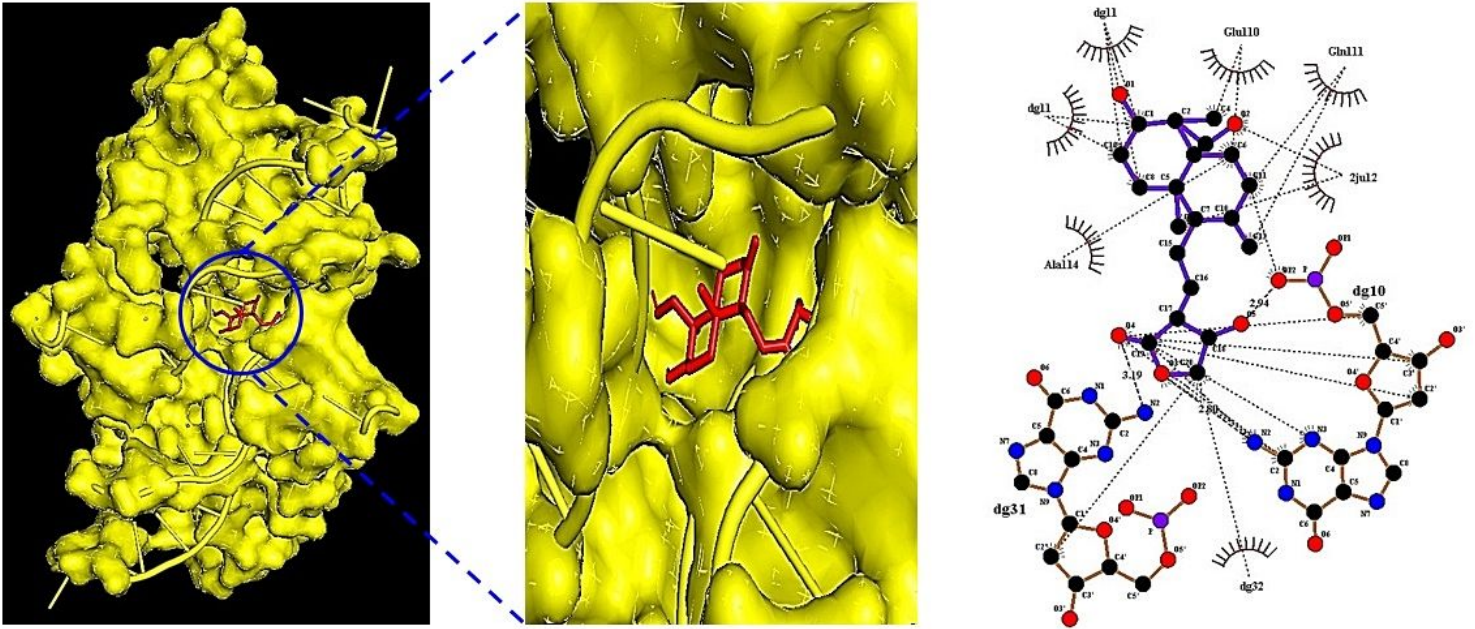


Figure 7

MDT of Andrographolide (PubChem ID: 5318517) on IL6 (PDB ID: 4NI9).

Supplementary Files

This is a list of supplementary files associated with this preprint. Click to download.

- [Graphicalabstract.docx](#)
- [SupplementaryTableS1.xlsx](#)
- [SupplementaryTableS2.xlsx](#)